RESEARCH ARTICLE

Longitudinal MRI quantification of muscle degeneration in Duchenne muscular dystrophy

Claudia Godi[1], Alessandro Ambrosi[2], Francesca Nicastro[3], Stefano C. Previtali[4], Corrado Santarosa[1], Sara Napolitano[5], Antonella Iadanza[1], Marina Scarlato[4], Maria Grazia Natali Sora[4], Andrea Tettamanti[3], Simonetta Gerevini[1], Maria Pia Cicalese[5], Clementina Sitzia[6], Massimo Venturini[7], Andrea Falini[1], Roberto Gatti[3], Fabio Ciceri[8], Giulio Cossu[9], Yvan Torrente[6] & Letterio S. Politi[1,10,11,12]

[1]Neuroradiology Department, Neuroradiology Research Group and CERMAC, San Raffaele Scientific Institute and Vita-Salute San Raffaele University, Milan, Italy
[2]CUSSB, University Centre for Biomedical Sciences, Vita-Salute San Raffaele University, Milan, Italy
[3]Laboratory of Analysis and Rehabilitation of Motor Function, Division of Neuroscience, San Raffaele Scientific Institute, Milan, Italy
[4] Division of Neuroscience, Institute of Experimental Neurology (INSpe), San Raffaele Scientific Institute, Milan, Italy
[5]San Raffaele Telethon Institute for Gene Therapy (HSR-TIGET) and Pediatric Immunohematology and Bone Marrow Transplantation Unit, San Raffaele Scientific Institute, Milan, Italy
[6]Stem Cell Laboratory, Department of Pathophysiology and Transplantation, Universitá degli Studi di Milano, Fondazione IRCCS Cá Granda Ospedale Maggiore Policlinico, Centro Dino Ferrari, Milan, Italy
[7]Radiology Department, San Raffaele Scientific Institute and Vita-Salute San Raffaele University, Milan, Italy
[8]Hematology and BMT Unit, San Raffaele Scientific Institute and Vita-Salute San Raffaele University, Milan, Italy
[9]Institute of Inflammation and Repair, University of Manchester, Manchester, United Kingdom
[10]Neuroimaging Research, Division of Hematology/Oncology, Boston Children's Hospital, Boston, MA, USA
[11]Department of Pediatrics, Harvard Medical School, Boston, MA, USA
[12]University of Massachusetts Memorial Medical Center and University of Massachusetts Medical School, Worcester, MA, USA

Correspondence

Letterio S. Politi, Neuroradiology Department, Neuroradiology Research Group and CERMAC, San Raffaele Scientific Institute and Vita-Salute San Raffaele University, Via Olgettina 60, 20132 Milan, Italy. Tel: +39 348 3221188; Fax: +39 02 2643 3447; E-mail: politi.letterio@hsr.it
and
Yvan Torrente, Stem Cell Laboratory, Department of Pathophysiology and Transplantation, Universitá degli Studi di Milano, Fondazione IRCCS Cá Granda Ospedale Maggiore Policlinico, Centro Dino Ferrari, via Francesco Sforza 35, 20122 Milan, Italy. Tel: +39 02 55033874; Fax: +39 02 55034723; E-mail: yvan.torrente@unimi.it

Abstract

Objective: The aim of this study was to evaluate the usefulness of magnetic resonance imaging (MRI) in detecting the progression of Duchenne muscular dystrophy (DMD) by quantification of fat infiltration (FI) and muscle volume index (MVI, a residual-to-total muscle volume ratio). **Methods**: Twenty-six patients (baseline age: 5–12 years) with genetically proven DMD were longitudinally analyzed with lower limb 3T MRI, force measurements, and functional tests (Gowers, 10-m time, North Star Ambulatory Assessment, 6-min walking test). Five age-matched controls were also examined, with a total of 85 MRI studies. Semiquantitative (scores) and quantitative MRI (qMRI) analyses (signal intensity ratio – SIR, lower limb MVI, and individual muscle MVI) were carried out. Permutation and regression analyses according to both age and functional test-outcomes were calculated. Age-related quantitative reference curves of SIRs and MVIs were generated. **Results**: FI was present on glutei and adductor magnus in all patients since the age of 5, with a proximal-to-distal progression and selective sparing of sartorius and gracilis. Patients' qMRI measures were significantly different from controls' and among age classes. qMRI were more sensitive than force measurements and functional tests in assessing disease progression, allowing quantification also after loss of ambulation. Age-related curves with percentile values were calculated for SIRs and MVIs, to provide a reference background for future experimental therapy trials. SIRs and MVIs significantly correlated with all clinical measures, and could reliably predict functional outcomes and loss of ambulation. **Interpretations**: qMRI-based indexes are sensitive measures that can track the progression of DMD and represent a valuable tool for follow-up and clinical studies.

Introduction

Duchenne muscular dystrophy (DMD) is a muscular disease caused by a mutation in the dystrophin gene that is responsible for a severe reduction or complete absence of protein expression.[1] This X-linked inherited disease affects one in 3600–6000 live male births.[2] The affected children undergo severe degeneration of skeletal myofibers,[3] with progressive loss of ambulation, cardiac and respiratory failure, and early death.[2] Despite to date no cure for DMD is available, many promising preclinical studies and clinical trials based on cellular and molecular therapies,[4] viral delivery of microdystrophin genes,[5,6] and exon skipping[7,8] have shown encouraging results in restoring the defective structure and function of myofibres in DMD animal models[9,10] and patients. Due to the high clinical variability of the disease, there is an urgent need for sensitive, objective, and reliable biomarkers to monitor disease progression and for validated outcome measures to evaluate the efficacy of these new therapeutic strategies in clinical trials. Clinical scores and timed tests such as North Star Ambulatory Assessment (NSAA) and 6-min walking distance test (6MWT) rely on patients' active collaboration, neuromuscular coordination and present a ceiling effect. Imaging techniques such as ultrasonography, computed tomography, or magnetic resonance imaging (MRI) have emerged to visualize structural and metabolic muscle pathologies. Muscle imaging also demonstrates dystrophic changes in clinically normal and affected muscles, suggesting that muscle MRI may become an important assessment tool in clinical trials involving patients with myopathies or myodystrophies.[11,12] However, most of the previous studies focused on semiquantitative assessment of muscle abnormality[13,14] and on reproducibility of quantitative MRI measures.[15] No longitudinal quantitative data are currently available on the progression of fat infiltration and atrophy in lower limbs of DMD patients, apart from a few studies only evaluating small subsets of muscles.[16–21] Furthermore, the contribution of individual muscles to the clinical performance has not been investigated.

This 4-year longitudinal study was designed to further evaluate the clinical usefulness and sensitivity of muscle MRI in detecting fibro-adipose degeneration in DMD with the focus on (1) semiquantitatively and quantitatively assessment of the compositional analysis of DMD patients' lower limb muscles in different age classes; (2) to provide age-related reference curves of fat infiltration and loss of volume in lower limb muscles of DMD patients through up to three different quantitative MRI measures, collected on a 4-year follow-up basis; (3) to correlate quantitative MRI markers of fat infiltration and loss of muscle volume to clinical scores, force measures, and timed tests, with the aim to disclose individual muscle contributions especially those difficult to assess clinically; (4) to assess the possibility of predicting loss of ambulation and of measuring disease progression after it.

Materials and Methods

Trial design and patients' selection

This is a longitudinal monocentric prospective study authorized by the Local Ethical committee, aimed to describe the natural history of patients affected by DMD.

In September to October 2009, the pediatric patients affected by DMD referred to our center were screened for inclusion criteria and consecutively enrolled. Inclusion criteria were as follows: proven DMD diagnosis (based on a clinical history of early onset, progressive muscle weakness, increased serum creatine kinase levels at least 10 times the upper limit of normal, absence of dystrophin on muscle biopsy, and genetic dystrophin analysis), preserved ability to ambulate without assistance at baseline, achievement of parents' written consent. Patients older than 13 years at baseline, enrolled in other experimental trials, or with any drug administration (except for steroids) were excluded from the study. The recruited patients were assessed clinically and with MRI of the lower limbs at the time of enrollment, then at nine to ten and at 24 months since baseline. Additional evaluations were performed, when allowed by the patients' compliance, at 36 and 48 months from the basal evaluation.

Functional measures

The clinical assessment of muscle strength, functional mobility, endurance and ability to walk included the 6MWT, the NSAA, the 10-m walk time (10-m time), and time to rise from floor. They were carried out as described previously.[22] All clinical tests were performed 1 day prior each MRI examination.

Force measures

One day before each MRI examination, two examiners performed patients' strength evaluation using the Kin Com® Robotic Dynamometer (Chattanooga Group Inc., Chattanooga, TN). The muscle groups tested were knee extensor and flexor, through isometric and isokinetic protocol, as previously described.[22]

MRI acquisition

All the subjects were imaged on a 3T scanner (Achieva 3T; Philips Healthcare, Best, The Netherlands) during the projection of a movie, without either sedation or contrast injection, with the "body coil" for transmission and reception. The scanning protocol consisted of axial T1-weighted spin echo (SE) sequences (slice thickness [THK] 4 mm; repetition time [TR] 550 ms; echo time [TE] 15 ms), axial T2-weighed Turbo SE sequences (THK 4 mm; TR 7300 ms; TE 90 ms), coronal Short Tau Inversion Recovery (STIR) T2-weighted sequences (THK 5 mm; TR 7100 ms; TE 70 ms; inversion time 200 ms), and coronal 3D THRIVE T1-weighted sequences (acquired voxel size 1.25/1.25/2.50 mm, reconstructed voxel size 1.25/1.25/1.25 mm, TR 4.2 ms, TE 2.1 ms), acquired separately on the hip, thigh regions, and on calves. The protocol duration was about 30 min.

Semiquantitative compositional analysis of lower limb muscles

All the MR images were scored in consensus by two neuroradiologists (L.S.P. and S.G., respectively, with 16 and 20 years of experience) with proficiency in neuromuscular diseases. For each patient, all the major muscles of the lower limbs were evaluated (44 muscles per patient in total). When atrophy, fat infiltration, edema, and hypertrophy were present, they were scored 1. A score ranging from 0 to 3 was given accordingly to the degree of fat infiltration (absent/mild/moderate/severe).

Quantitative analysis of lower limb muscles

Signal intensity ratio

A 5-year experienced single operator (C.G.) manually outlined the areas of knee extensors (quadriceps), knee flexors (biceps femoris, semitendinosus, and semimembranosus), sartorius, gracilis, and gluteus maximus muscles of both sides on axial T1-weighted images. The signal intensity from each region of interest (ROI) was normalized to the nearby subcutaneous fat, obtaining a signal intensity ratio (SIR) to measure fat infiltration. For thigh muscles, the final SIR was averaged among five slices covering the whole length of the femur.

Lower limb segmental muscle volumes

On axial T1-weighted images a single operator (C.G.) manually segmented the thighs and legs volumes on a dedicated workstation (Advantage Workstation, General Electrics Healthcare, Milwaukee, WI). The anatomical landmarks for segmentation of the volume of interest were the intertrochanteric line and the distal femoral metaphysis for the thigh, and the proximal and distal tibial metaphyses for the leg. After applying a signal intensity threshold (50–160) to select unaffected muscle tissue, the volume of the thresholded muscle was normalized to the segmented thigh and leg volumes, to obtain thigh and leg muscle volume percentage index (MVI).

Individual muscle volumes

The volumes of quadriceps, biceps, semitendinosus, semimembranosus, sartorius, gracilis, soleus, and gastrocnemius of both limbs were generated on axial T1-weighted images through a semiautomated system using the software Amira® (FEI Visualization Sciences Group, Hillsboro, OR, USA). A ROI was drawn for each of the above-mentioned muscles by a single operator, and manual segmentation was repeated every three slices along the full muscle length. For each muscle, the muscle volume within its sheath was obtained through software generated interpolation of the traced ROIs and manual correction. A fat-normalized threshold was then applied to measure the unaffected muscle tissue within the sheath. This value was eventually normalized to the former value, obtaining relative individual volumes of spared muscular tissue for each muscle.

Statistical analyses

Statistical analyses were performed with SPSS 18.0 (IBM, Armonk, NY, USA), Prism (GraphPad Software, La Jolla, CA, USA) and R environment (www.r-project.org). Observed numeric values were reported by means of median and range.

For each muscle, MVI trend as function of age was analyzed fitting quantile regression models based on natural spline functions with degrees of freedom chosen by means of cross validation. To give an overall picture of both the trend and the data variability, we fitted the quantile regression models corresponding to the 5th, 10th, 25th, 50th (median), 75th, 90th, and 95th percentiles.

We analyzed Gowers and 10-m time values as function of MVI and SIR values fitting nonlinear exponential models with nested random effect on subject and limb to take account of the dependencies between observations, separately for each muscle. Since there was no evidence of nonlinearity, we fitted a linear mixed effect model, with nested random effect on subject and leg, to investigate the pattern of 6MWT and NSAA as function MVI and SIR.

Spearman's correlation coefficients were also computed between variables. Differences between groups were

verified by means of the Mann–Whitney test statistic. Exact *P*-values computed by means of permutations to avoid any distributional assumption or asymptotic approximation. *P*-values <0.05 were considered significant.

Results

Population

Twenty-six ambulant DMD patients (14 on daily steroids, 11 on intermittent steroids, one without steroid therapy) fulfilled the inclusion criteria and were enrolled in the study.

The recruited patients ranged from 5 years and 10 months to 14 years and 2 months of age at last MRI acquisition, with median value at baseline of 8 years and 9 months (baseline range: 5–12 years). According to the age at baseline, patients were grouped into three classes: 5–7, 8–9, 10–12-year-old children, respectively, of 7, 11, and 8 boys each. During the follow-up, loss of ambulation occurred in 6 of 26 patients.

Two of the 26 patients were lost after baseline, and two of the remainder dropped out after the first follow-up scan: in total, 22 of 26 patients completed at least three clinical and MRI evaluations. Additional fourth and fifth assessments were available, respectively, for 6, and 5, of the 22 boys, with a clinical and imaging follow-up up to 4 years.

Age at enrollment, type of mutation of the dystrophin gene and 6MWT distance at enrollment of each DMD patient are shown in Table 1.

Five healthy boys (median age: 11 years and 2 months; age range: 9 years and 5 months – 13 years) who underwent the same clinical and imaging protocol in that period were included for comparison. Overall, 85 MRI studies of the lower limbs were performed. All subjects demonstrated a good compliance with MRI despite no sedation, thanks to the movie projection with a minimal drop out at follow-up scans, confirming the feasibility of the MRI assessment.

Semiquantitative compositional analysis of DMD lower limb muscles

At baseline cross-sectional assessment, in the youngest age class (5–7-year-old) fat infiltration was seen on T1-weighted images in almost all patients in maximus and medius gluteus and magnus adductor. The tensor fasciae latae, rectus femoris, biceps, and semimembranosus were also involved with a lower prevalence (Fig. 1A and B, blue histograms). Fat infiltration became progressively more severe in middle-aged patient class (8–9-year-old, Fig. 1A and B, red histograms) and also involved longus

Table 1. Age at enrollment, type of mutation of the dystrophin gene and 6-min walking test distance at enrollment of all Duchenne muscular dystrophy patients.

Subject	Age at enrollment (years)	Mutation type	6-min walking test at enrollment (m)
01	7	Del. ex 51–53	281
02	6	Point Mut. ex 43	360
03	9	Del. ex 19,43,44	348
04	8	Del. ex 45,46,47	505
05	10	Del. ex 48–52	303
06	9	Del. ex 48–52	343
07	7	Del. ex 4–44	405
08	9	Del. ex 3–12	331
09	8	Del. ex 45–50	311
10	11	Del. ex 47–52	225
11	12	Del. ex 3–7	46
12	9	Point Del. ex 59	391
13	8	Del. ex 50 + Heterozygous Del. SMN1	344
14	10	Duplication ex 2	469
15	9	Del. ex 50	297
16	7	Del. ex 52	350
17	9	Del. ex 16–17	380
18	11	Del. ex 51	382
19	5	Del. ex 54	374
20	11	Del. ex 45–50	394
21	8	Promoter Del.	389
22	7	Point Mut. ex 54	407
23	7	Unknown	75
24	10	Del. ex 45	327
25	8	Del. ex 50–52	325
26	10	Del. ex 50–52	90

Del, deletion; ex, exon; Mut, mutation.

adductor, lateral, intermediate, medial vasti, gastrocnemius, soleus, and peronei muscles. Minimus gluteus and obturatores, semintendinosus, sartorius, gracilis, and posterior tibialis were affected only in the oldest children (10–12-year-old, Fig. 1A and B, green histograms). Atrophy was demonstrated in hip and thighs since the age of 8–9: gluteus maximus, quadriceps and biceps femoris were the most involved muscles in terms of atrophy prevalence. On the contrary, no atrophy was seen in the leg (Fig. 1C). Conversely, hypertrophy was present since the age of six mainly in the calf muscles (gastrocnemius, soleus, and anterior tibialis) and in gracilis, with a later involvement of sartorius, adductor longus, and peronei muscles since the age of 8 (Fig. 1D). Edema was best seen on T2 STIR images, mainly in the soleus muscle and in the youngest patients (Fig. 1E). Atrophy and fat infiltration were progressive in the three patient classes, whereas edema was a fluctuant finding and could appear or disappear over time (Fig. 1, right column histograms).
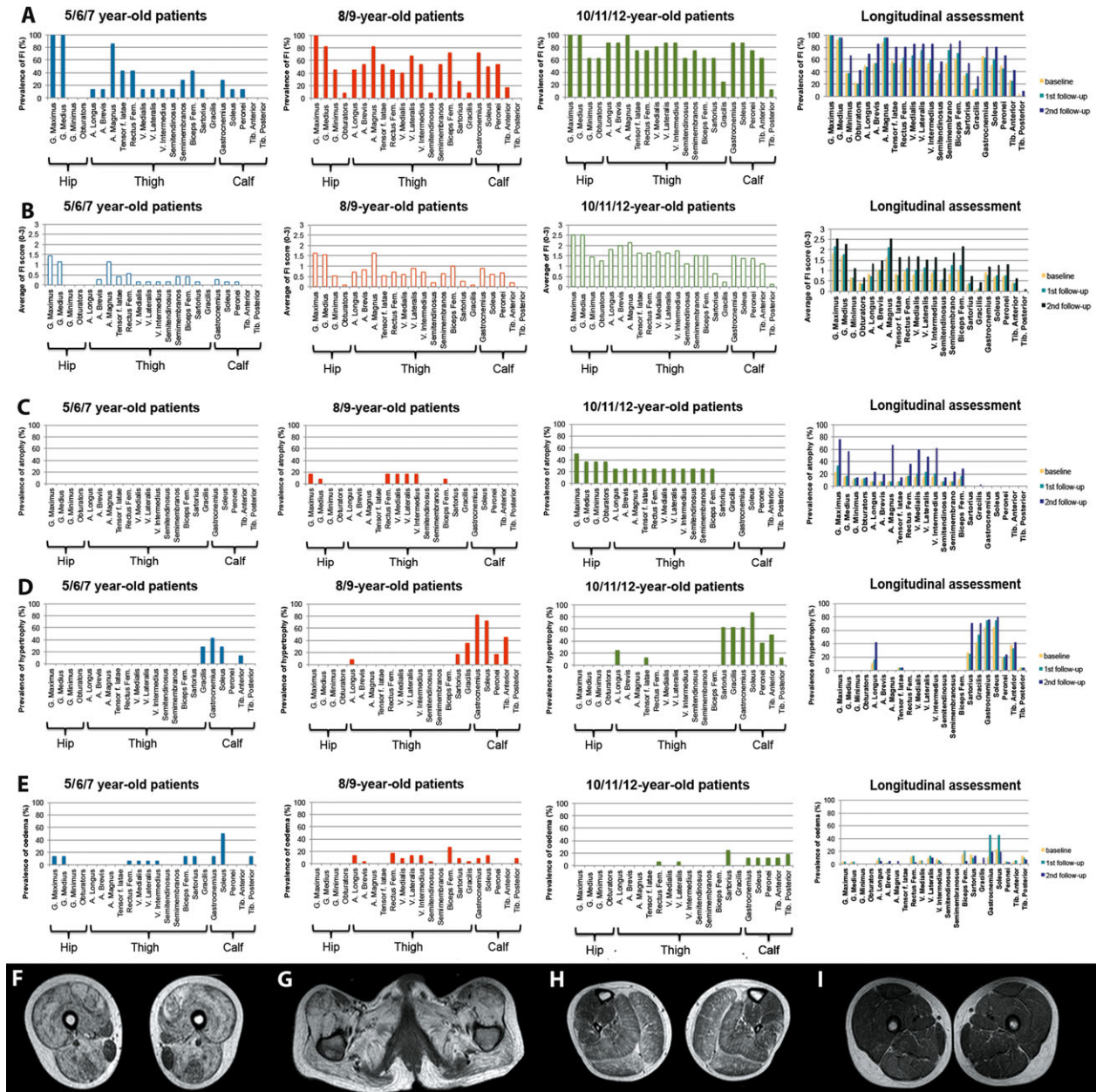
Figure 1. Semiquantitative compositional analysis of lower limb muscles. Muscles of hip and both lower limbs were scored at baseline and during follow-up to assess the presence of fat infiltration, atrophy, hypertrophy, and edema (0: absent, 1: present). An additional four-points score (0: absent – 3: severe) was attributed to grade the severity of fat infiltration. Baseline cross-sectional assessment of prevalence of fat infiltration (A), severity of fat infiltration (B), prevalence of atrophy (C), hypertrophy (D), and edema (E) in patients of different age groups are reported in the first three columns. In the right column, longitudinal modifications of these parameters are shown. Representative axial T1-weighted images showing fat infiltration of thigh muscles (F), atrophy of glutei muscles (G), and hypertrophy of calf muscles (H) are reported. In (I) an axial T2-weighted image shows edema in thigh muscles. Fat infiltration prevalence (A) was more prominent at baseline in the hip and thigh of 5–7-year-old patients with involvement of the calf muscles at the age of 8–9 and of obturators, sartorius, and gracilis at the age of 10–12. The severity of fat infiltration almost paralleled the prevalence of fat infiltration (B). Atrophy (C) was evident mainly in the hip and thigh of the eldest subjects, whereas hypertrophy and edema (D and E, respectively) were present mostly in the calf. All the above-mentioned parameters progressed over time (right column: follow-up evaluation), except for edema.

Quantitative analysis of lower DMD limb muscles

Signal intensity ratio

At baseline, in DMD patients the SIRs of all analyzed muscles, apart from sartorius and gracilis, were higher than in normal controls (Fig. 2), due to fat infiltration that is responsible for signal increase in the T1-weighted images. The highest SIRs were found on glutei muscles, followed by quadriceps and knee flexors. In addition, DMD patients' glutei, flexors, quadriceps SIRs showed progressive increase according to age class. Gracilis and sartorius SIRs remained stable among all the age classes.

Individual patients' SIRs remained stable or increased along time in the follow-up the assessments. A significant SIR increase over time was demonstrated in each age class.

A significant SIR increase was observed also in the six patients that became wheel chair-bound during the follow-up, even after the loss of ambulation (Fig. S1A). ROC curves and cut-off values of SIRs for discrimination of ambulation ability are reported in Figure S2A and B and in Table 2, respectively.

Lower limb segmental muscle volumes index

All patients' age groups – apart from the 5–7-year-old boys – had baseline thigh MVIs and leg MVIs significantly lower than healthy controls (*P*-value <0.05, Fig. 3) due to fatty degeneration. The thigh MVI, but not leg MVI, significantly decreased in accordance to age class (*P*-values <0.05, except for thigh MVI of 8–9-year-old boys to 10–12-year-old boys, *P*-value = 0.06). A significant decrease over time of thigh MVI, but not of leg MVI, was demonstrated in each age group. A significant decrease in thigh MVI was observed also in nonambulant patients (Fig. S1B). ROC curves and cut-off values of MVIs for discrimination of ambulation ability are reported in Figure S2C and D and in Table 2, respectively.

Individual muscle MVI

At baseline, in every age group, all the patients' individual muscle volume indexes (quadriceps, biceps femoris, semitendinosus, semimembranosus, gracilis, sartorius, gastrocnemius, and soleus) were significantly lower than healthy
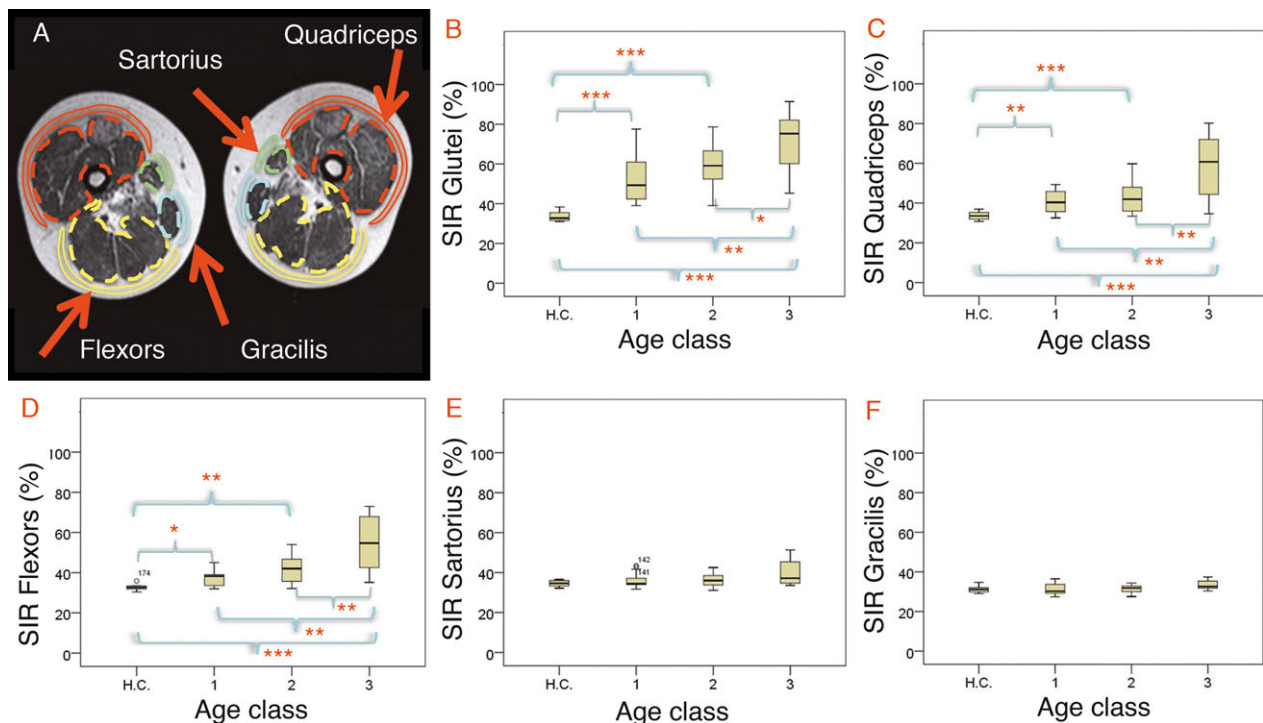

Figure 2. Signal Intensity Ratios of hip and thigh muscles. At baseline examination, fat infiltration of the gluteus maximus, quadriceps, flexors, sartorius, and gracilis muscles was quantified bilaterally as a signal intensity ratio (SIR) between muscle signal intensity and the signal intensity of the nearby subcutaneous fat (A). Duchenne muscular dystrophy (DMD) patients were grouped into three classes, according to their age at baseline (1: 5–7-year-old patients; 2: 8–9-year-old patients; 3: 10–12-year-old patients). Mean SIR from gluteus maximus (B), quadriceps (C), and flexors (D) was significantly higher in DMD patients than in normal healthy controls. These mean SIRs of DMD patients significantly increased along with the age group. Conversely, no difference in mean SIR was ever appreciable for sartorius (E) and gracilis (F). H.C., healthy controls.

Table 2. Cut-off values of muscle degeneration allowing discrimination between ambulant and nonambulant patients.

Parameter	Cut-off	Sensitivity (%)	Specificity (%)	PPV (%)	NPV (%)	Accuracy (%)
SIR quadriceps	77.70	80	95	80	95	92
SIR flexors	69.50	100	95	83	100	96
Thigh MVI	13.35	100	90	71	100	92
Calf MVI	32.96	100	81	55	100	85
Biceps MVI	8.00	100	95	83	100	96
Soleus MVI	45.00	100	100	100	100	100

SIR, signal intensity ratio; MVI, muscle volume index; PPV, positive predictive value; NPV, negative predictive value.
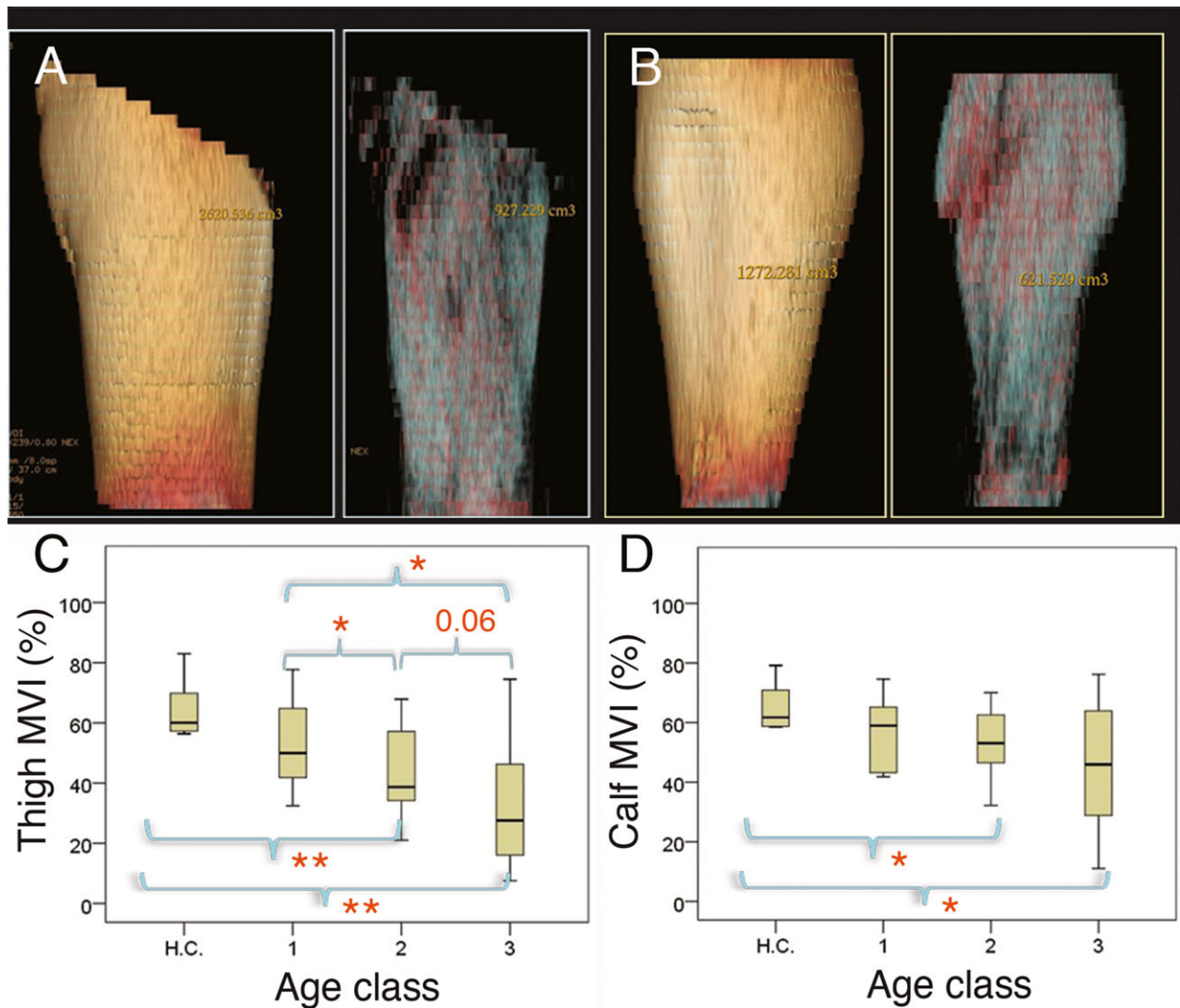

Figure 3. Lower limb segmental muscle volume index. At baseline evaluation, the percentage of spared muscular volumes of thighs and calves were expressed as muscle volume index (MVI), a ratio between the preserved muscular volume (A and B, right image) and the whole thigh/calf volume (A and B, left image). Duchenne muscular dystrophy (DMD) patients were grouped into three classes, according to their age at baseline (1: 5–7-year-old patients; 2: 8–9-year-old patients; 3: 10–12-year-old patients). Mean thigh (C) and calf (D) MVI from all DMD patients, except for the 5–7-year-old group, were significantly lower than healthy controls' ones. A significant decrease in thigh MVI in DMD patients was also detected with the increase of the age class. H.C., healthy controls; MVI: muscle volume index.

controls (Fig. 4). Although individual muscle volumes decreased along with the increase in the age class, differences among groups were not significant, except for semimembranosus muscle (*P*-values <0.01). A difference in semitendinosus and biceps volume was also shown between the 10–12-year-old group and, respectively, the

5–7-year-old group and the 8–9-year-old group (*P* < 0.05). A nonsignificant difference, yet with *P*-value (0.6–0.7) just above statistical significance, was found among the same age groups for quadriceps and gastrocnemius muscle volumes. Finally, a decrease in biceps muscle volume with an associated *P*-value just below statistical
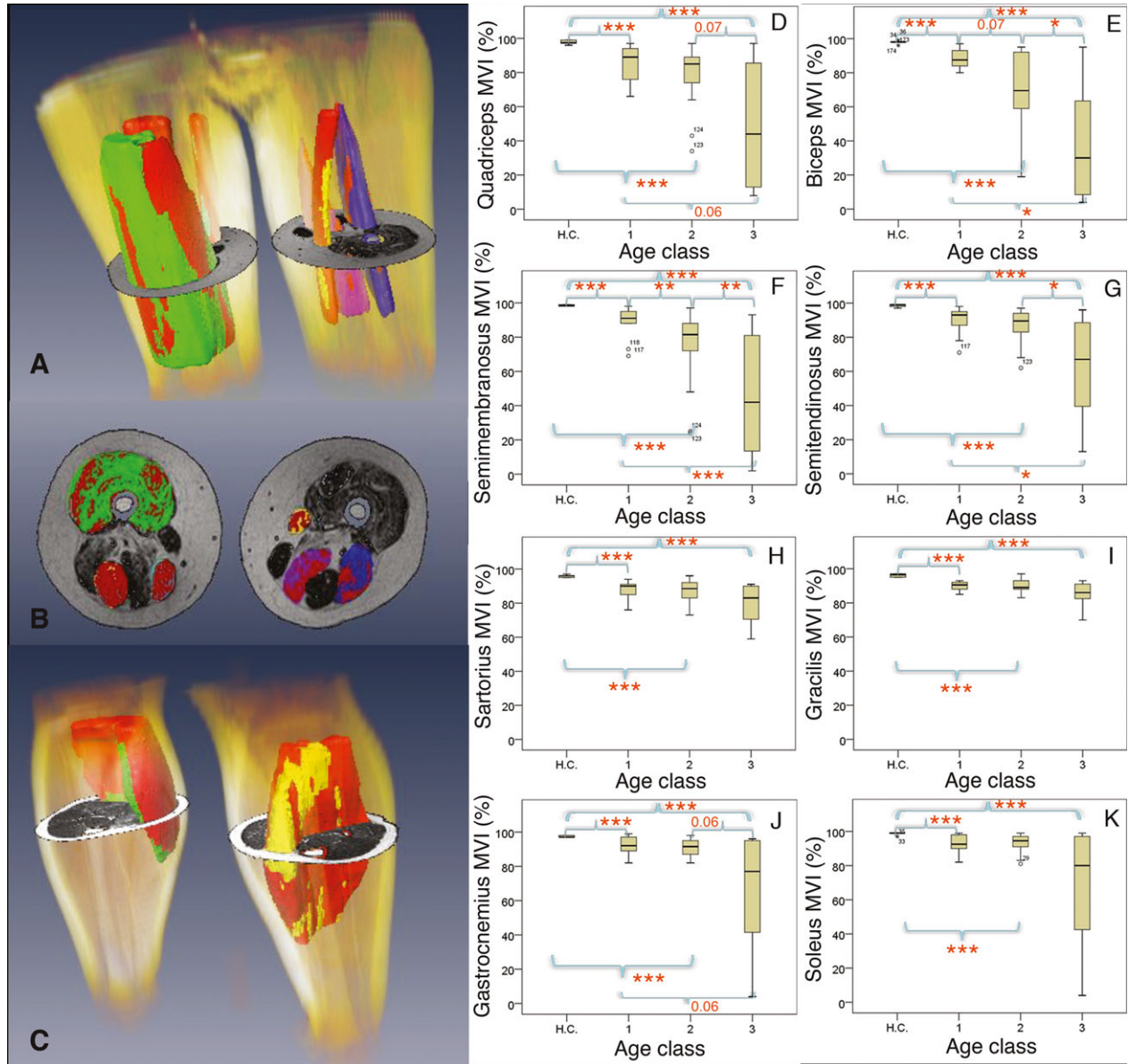

Figure 4. Quantitative individual muscle volume index. Individual muscle volumes were measured by semi-automatically contouring muscle sheaths on axial Spin Echo T1-weighted images. A threshold to select preserved muscle tissue was then applied within the outlined sheath volume. A ratio between the individual muscular intrasheath volume and the threshold volume was calculated to get a Muscle Volume Index (MVI, A–C). Duchenne muscular dystrophy (DMD) patients were grouped into three classes according to their age at baseline (1: 5–7-year-old patients; 2: 8–9-year-old patients; 3: 10–12-year-old patients). DMD patients' mean MVI was significantly lower than healthy controls' one for every tested muscle (quadriceps (D), biceps (E), semimebranosus (F), semitendinosus (G), sartorius (H), gracilis (I), gastrocnemius (J), and soleus (K)), and for all age groups. Ten- to twelve-year-old DMD patients showed biceps (E), semimebranosus (F), and semitendinosus (G) MVIs significantly lower than the 5–7- and 8–9-year-old groups. Semimembranosus (F) MVI in the 8–9-year-old group was also significantly lower than in the 5–7-year-old one. H.C., healthy controls; MVI, muscle volume index.

significance (0.07) was also demonstrated between 6–7-year-old and 8–9-year-old groups. Over time, a significant decrease in individual muscle volume was shown in each age class. Representative MRI images acquired longitudinally on the same patient are reported in Figure 5.

A significant MVI decrease was observed also in the six patients that became wheel chair-bound during the follow-up, even after the loss of ambulation (Fig. S1C). ROC curves and cut-off values of individual muscles MVIs for discrimination of ambulation ability are reported in Figure S2E–F and in Table 2, respectively.

Age-related reference curves of SIRs and MVIs in lower DMD limb muscles

The 5th, 10th, 25th, 50th (median), 75th, 90th, and 95th percentiles of SIRs, thigh and leg MVIs, and individual muscle volumes, collected on a 4-year follow-up basis, were calculated and then plotted relative to time (patients' age). Glutei muscle SIRs showed a shallow progression, corresponding to long-standing fat infiltration. Quadriceps and knee flexor SIRs had a steeper, similar rate of increase over time (Fig. 6B, D and G). Notably, between 5 and 8 years of age, the median values of the SIRs of the glutei, flexors and of the quadriceps increased in a slightly steeper way that the median NSAA, shown as reference (Fig. 6A and G). Sartorius and gracilis demonstrated the lowest SIR values, and a more flat and modest progression than the former muscles in the examined time frame (Fig. 6E and F).

The loss of volume was faster for thigh than for leg MVI. A decline in leg MVI was evident only after the age of 10. In individual muscle volumes, the rate of volume loss was similar in quadriceps, biceps, and semimembranosus muscles (Fig. 7A–C and I). The median values of
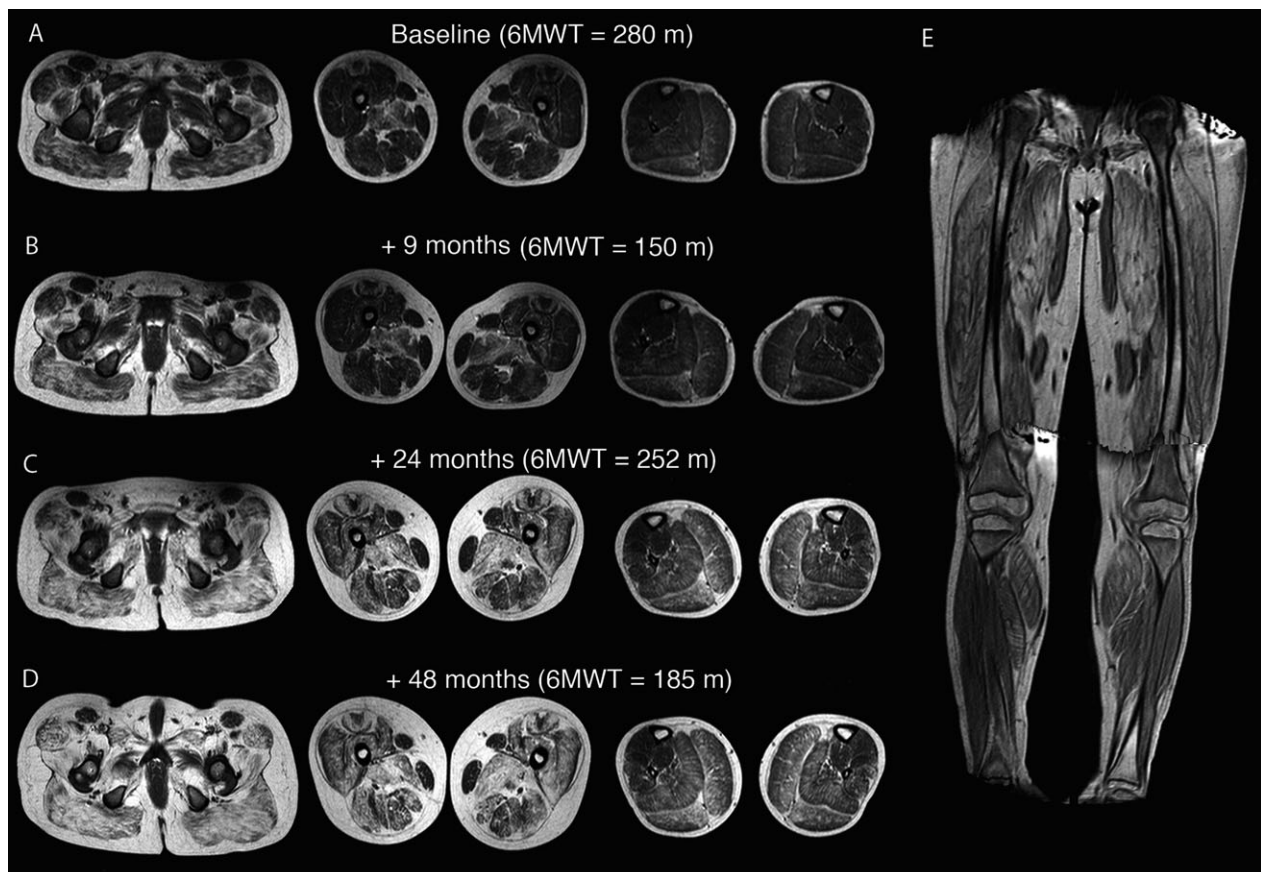

Figure 5. Representative MRI images acquired longitudinally on the same patient. A-D) Axial Spin Echo T1-weighted images of glutei (left column), thighs (middle column), and calves (right column) from a Duchenne muscular dystrophy patient at different time points (A, B, C, D). Please notice the progression over time of atrophy in thighs, hypertrophy in calves, and fat infiltration in both thighs and calves. A representative coronal view of 3D THRIVE from the same patient is also shown in E. 6MWT distance measured 1 day prior to each MRI examination is reported for reference. The patient preformed a higher distance in C than in B, due to the lack of active collaboration. 6MWT: 6-min walking test.

the MVIs of these muscles declined between 5 and 8 years of age; in the same age range no decline in the 6-min walking test performance, Gowers, 10-m time, NSAA and force measurement was registered (Figs. 7I and S3). Semi-tendinosus, soleus, and gastrocnemius muscles showed a slower volume decay, becoming more conspicuous after the age of 10 (Fig. 7D, G and H) Sartorius and gracilis had the most delayed loss of volume among the lower limb muscles, still unremarkable, respectively, by the age of 11 and 12 (Fig. 7E and F).

Only the median value of the SIRs of the glutei, flexors and the quadriceps, and of the MVIs of biceps, quadriceps, and semimembranosus muscles (and not clinical tests and force measures) were significantly ($P < 0.05$) modified between 5 and 8 years of age, being the biceps and quadriceps MVIs significantly reduced every year.

Furthermore, the variability in SIR and MVI measures among different patients (see 5th and 95th percentile lines in Figs. 6B–F and 7A–H, respectively) was lower than that presented by clinical tests and force measures (Figs. 6A and S3). As a matter of fact, the statistical dispersion of clinical tests and strength measures in terms of both interquartile ranges (IQR) and median absolute deviations (MAD) was higher than that of MRI-derived quantitative measures (Table 3).

Clinical scores and timed-test: correlation and regression analyses to SIRs and MVIs

Overall, NSAA, 6MWT, Gowers, and 10-m time showed a significant correlation with SIRs, thigh and leg MVIs and individual muscle volumes (Spearman ρho: 0.5–0.8, *P*-values <0.05). Only the correlation of clinical scores to sartorius and gracilis SIRs and to their volumes was fair to poor (Spearman ρho: 0.2−0.5) and sometimes did not reach statistical significance. The best correlation was found for NSAA and quantitative MRI measures (particularly quadriceps and knee flexors volumes and SIRs, thigh and leg MVIs) with Spearman ρho of 0.7–0.8 and *P*-values <0.01 (Fig. 8). An inverse function of MVI was found to predict Gowers and 10-m time test values. For any thigh MVI, associated Gowers and 10-m time test were always worse than for the same leg MVI value. In addition, three clusters of individual muscle volumes with similar behavior in predicting 10-m time value were identified: biceps, semimembranosus and quadriceps as the first cluster, semitendinosus, gastrocnemius and soleus intermediately, sartorius, and gracilis as the last cluster. A similar pattern was also displayed for Gowers, with gastrocnemius and soleus muscle volumes in the third cluster with sartorius and gracilis muscles. Muscle volumes linearly predicted NSAA and 6MWT, with the same order as in Gowers and 10-m time (biceps and gracilis MVIs,

respectively, associated with the worst and the best clinical outcome). SIRs predicted the value of timed tests (Gowers and 10-m time) in a nonlinear fashion, and NSAA and 6MWT in a linear way. For any of the functional tests, glutei SIRs always predicted the worst clinical performance, followed, respectively, by knee extensors, flexors, sartorius, and gracilis SIRs.

Discussion

This is the longest and one of the largest longitudinal study with MRI, clinical tests, and force measures in DMD patients. Our study demonstrates that quantitative MRI values of fat infiltration and muscle volumes are sensitive and objective measures, able define the disease progression even after loss of ambulation, and correlate with clinical performances measured with NSAA, 6MWT, Gowers, and 10-m time.

Fatty degeneration is a feature of dystrophic myopathies. Muscle MRI is frequently applied in biopsy targeting to localize inflammatory alterations or subtle alterations of muscles or muscle groups that can be detected more easily with MRI than with clinical examination. MRI of the whole body may additionally visualize specific patterns of muscle involvement. Thus, increasing evidence supports the use of MRI as a tool to assess both the patterns and degrees of muscular involvement in a one-stop-shopping concept.[23] MRI may provide a valuable anatomical supplement to functional muscle testing. In our study, semiquantitative scores given to MRI images demonstrated that DMD progressively involves different muscle groups with a characteristic proximal to distal pattern of progression over time that is usually highly replicated in all patients. Fat infiltration starts with early involvement of glutei and adductors, less severely biceps and semimembranosus muscles in the youngest steroid-treated boys (5–7-year-old). At that age, early but less severe infiltration is also demonstrated on the posterior calf (gastrocnemii and soleus), in agreement with the results of nonsteroid-treated patients of Schreiber et al.[11] By the age of 8–9, infiltration of quadriceps and peroneus muscles can be observed. Sartorius, gracilis, and tibialis muscles are usually involved only in the late stage of the disease. Edema mostly involved the muscles spared by fat infiltration with an almost unpredictable pattern, in accordance to the features described by Marden et al.;[24] thus, its quantification was not considered useful to mark disease progression in this study, despite discloses an inflammatory status that might suggest adjustment of the steroid regimen. Atrophy is delayed in comparison to fat infiltration, but presents the same proximal-to-distal distribution, with sparing, and even apparent hypertrophy of gracilis, sartorius, and calf muscles, confirming what has already been described by other authors.[24]
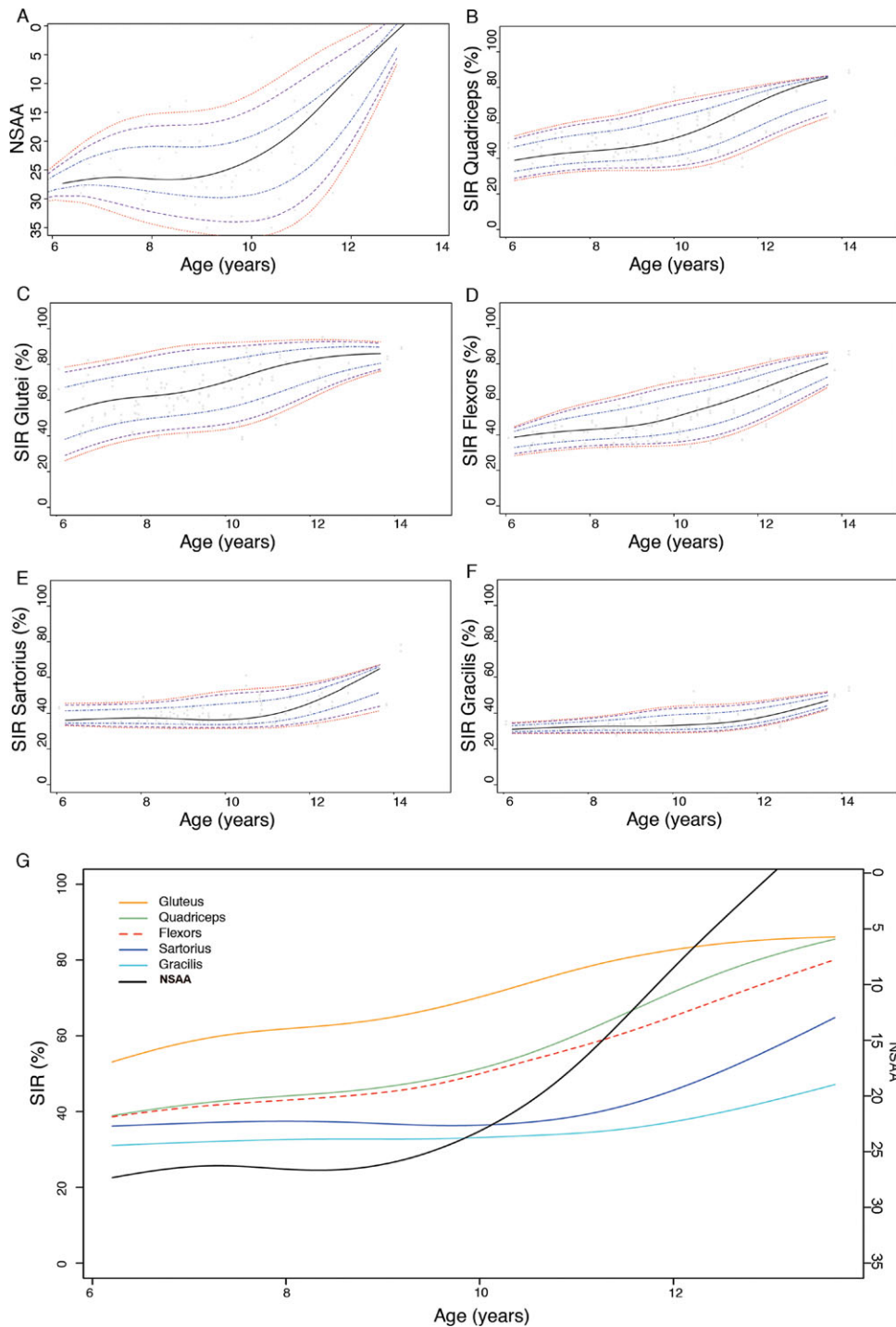
Figure 6. Age-related reference curves of SIRs. Age-related quantiles were calculated and plotted for NSAA (A) as reference, and for quadriceps (B), glutei (C), flexors (D), sartorius (E), and gracilis (F) SIRs. SIRs were constantly progressing in all muscles, except for sartorius and gracilis, which were not compromised before the age of 11. Representative 50th percentile SIR curves are reported on the large graph at the bottom (G), to compare the progressive infiltration of different muscles over time. Please note that between 5 and 8 years of age, the median values of the SIRs of the glutei, flexors, and of the quadriceps increased in a slightly steeper way that the median NSAA. Notably, the variability in SIR measures among different patients (see 5th and 95th percentile lines in B-F) was lower than that presented by NSAA (A). SIR, signal intensity ratio; NSAA, north star ambulatory assessment.
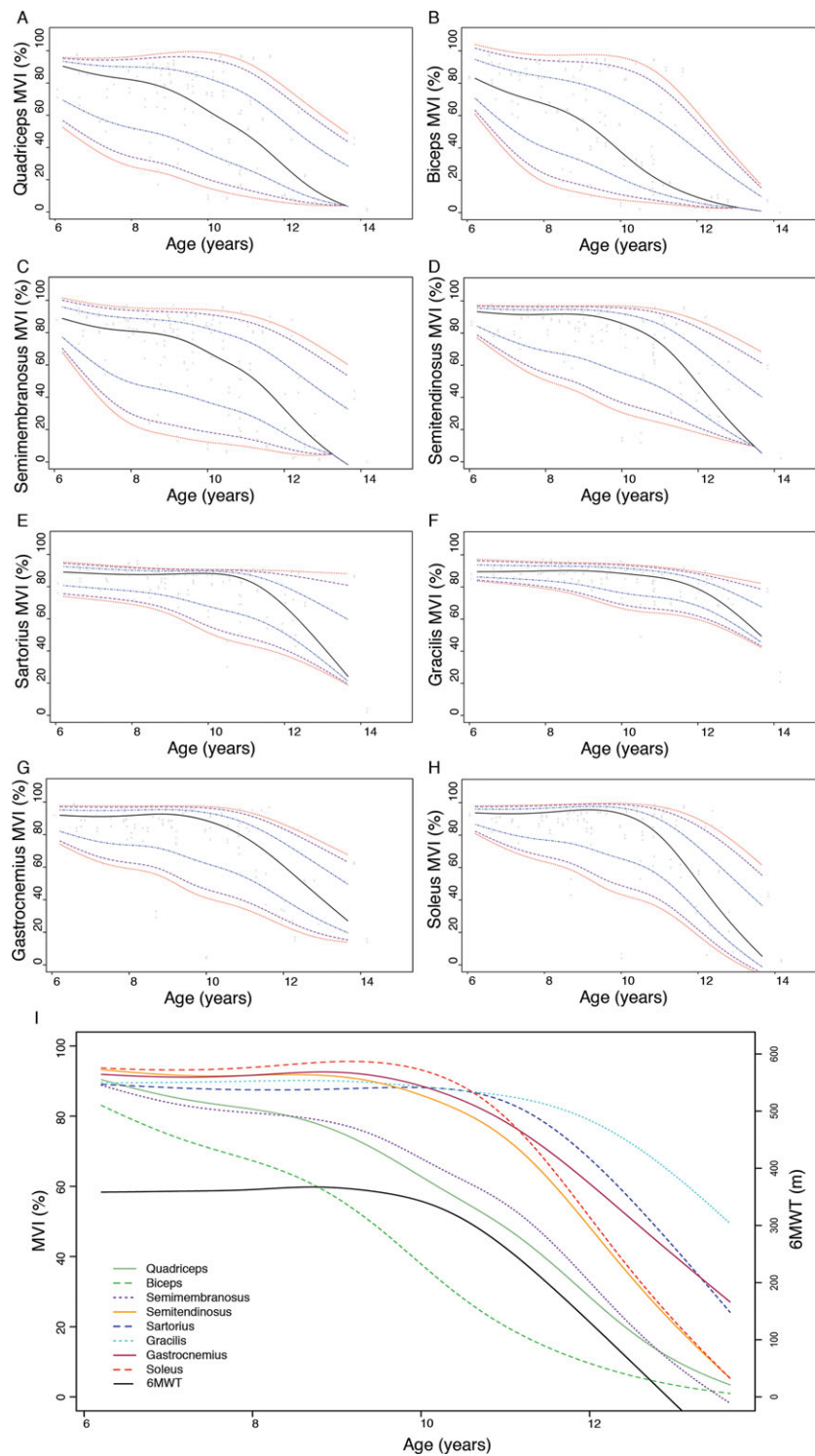
Figure 7. Age-related reference curves of MVIs. Age-related quantiles were calculated and plotted for quadriceps (A), biceps (B), semimembranosus (C), semitendinosus (D), sartorius (E), gracilis (F), gastrocnemius (G), and soleus (H) MVIs. MVIs were constantly decreasing in all muscles, except for sartorius and gracilis (E and F), which remained stable and started to decline at the age of 11. Representative 50th percentile MVI curves are reported on the bottom graph, to compare the loss of volume of different muscles over time (I), showing median 6MWT as reference (black line). Please note that between 6 and 8 years of age, median values of the MVIs of biceps, quadriceps, and semimembranosus muscles declined, whereas no decline was evident in the median 6MWT. MVI, muscle volume index; 6MWT, 6-min walking test.

Table 3. Variability among patients of force measures, clinical tests, and MRI quantitative parameters expressed as interquantile range and median absolute deviation. Please note that both SIR and MVI present a markedly lower variability in comparison to force and clinical measures.

	Interquantile range	Median absolute deviation
Isometric extension	33.36	22.17
Isometric flexion	27.26	22.70
Isokinetic extension	30.89	20.70
Isokinetic flexion	19.44	14.88
NSAA	7.69	5.86
6MWT	85.23	60.37
10 m time	2.70	2.00
Gowers	7.56	5.42
MVI THIGH	0.21	0.13
MVI LEG	0.17	0.12
MVI extensors	0.33	0.21
MVI sartorius	0.11	0.06
MVI gracilis	0.07	0.05
MVI biceps	0.32	0.19
MVI semitendinosus	0.17	0.13
MVI semimembranosus	0.29	0.21
MVI gastrocnemius	0.14	0.09
MVI soleus	0.13	0.09
SIR glutei	0.18	0.14
SIR extensors	0.14	0.10
SIR flexors	0.10	0.07
SIR sartorius	0.07	0.04
SIR gracilis	0.04	0.02
Mean strength measures	**27.74**	**20.11**
Mean clinical tests	**25.80**	**18.41**
Mean MVI	**0.19**	**0.11**
Mean SIR	**0.10**	**0.07**

SIR, signal intensity ratio; MVI, muscle volume index; NSAA, North Star Ambulatory Assessment; 6MWT, 6-min walking distance test.
Bold values in table 3 (the last four lines) are the mean of each category that are reported in detail above.

Although easily approachable, MRI visual scores are subjective and can often underestimate or overrate muscle abnormalities; thus these scores are not able to define the natural history of the disease, neither to highlight subtle changes in muscles that could be useful in future clinical trials. T1 SIR increases with the content of hyperintense fat components within the muscle tissue inside the fascia, and thus can be employed as a surrogate marker of adipose degeneration. T1 SIRs have already been employed in several small studies on DMD patients for quantification of fat infiltration[16,17] and its accuracy and repeatability have already been assessed.[12,25] The changes in measure of fat infiltration observed in our study quantitatively confirm that glutei and knee flexors are the most frequently and the most severely affected among hip and thigh muscles in DMD patients, even in the early stages, followed by

quadriceps. Sartorius and gracilis show the lowest fat infiltration values among lower limb muscles, with SIRs that are comparable to healthy controls' muscles in all examined age classes. SIR of all examined muscles, except for sartorius and gracilis, were significantly higher than controls even in the youngest class age (5–7), suggesting a high sensitivity for fat degeneration of this technique.

Since volumes better correlated with muscle mass and torque[26–28] than cross-sectional areas, in our study the volume percentage of muscle tissue within normal signal range was quantified with both segment-limb volume approach (thigh and calf MVIs) and individual muscle approach (individual muscle MVIs). Despite more sophisticated techniques are now available for measuring percentage of fat infiltration in DMD patients' muscles, such as three-point Dixon acquisitions,[29,30] our technique is sensitive and can be easily determined from conventional Spin Echo T1 imaged that can be acquired in all MR scanners within few minutes. Overall, quantitative muscle volume measures are consistent with atrophy semiquantitative findings and with T1 SIRs quantitative measures. Interestingly, muscle volume quantification permitted to appreciate even subtle volume changes – like mild loss in the soleus and gastrocnemius volumes in the oldest boys – that could become important during the assessment of efficacy of new treatments. As shown in the Figure 7I, the median values of the MVIs of the biceps, quadriceps and semimembranosus decline between 6 and 8 years of age; in the same age range no decline in the 6MWT, Gowers, 10-m time, NSAA and force measurement was registered (see also Fig. S3). As a matter of fact, only the median value of the SIRs of glutei, flexors, and quadriceps, and of the MVIs of biceps, quadriceps, and semimembranosus (and not clinical tests and force measures) were significantly ($P < 0.05$) modified between 5 and 8 years of age, being the biceps and quadriceps MVIs significantly reduced every year. Therefore the MRI-derived parameter MVI of biceps and quadriceps can be considered an early marker of disease progression since its variations can precede clinical decline and thus are more effective than clinical tests in detecting disease progression in this timeframe.

Furthermore, the variability in SIR and MVI measures among different patients was lower than that presented by clinical tests and force measures. Therefore, MRI measures could be used as sensitive end points for measuring disease-modified effects of new treatments within clinical trials allowing reduction in the number of patients required to demonstrate efficacy.

This study provided quantitative data that permitted the elaboration of MRI reference curves of fat infiltration and muscle volume for DMD patients, inspired to those used by pediatricians to monitor children's height,
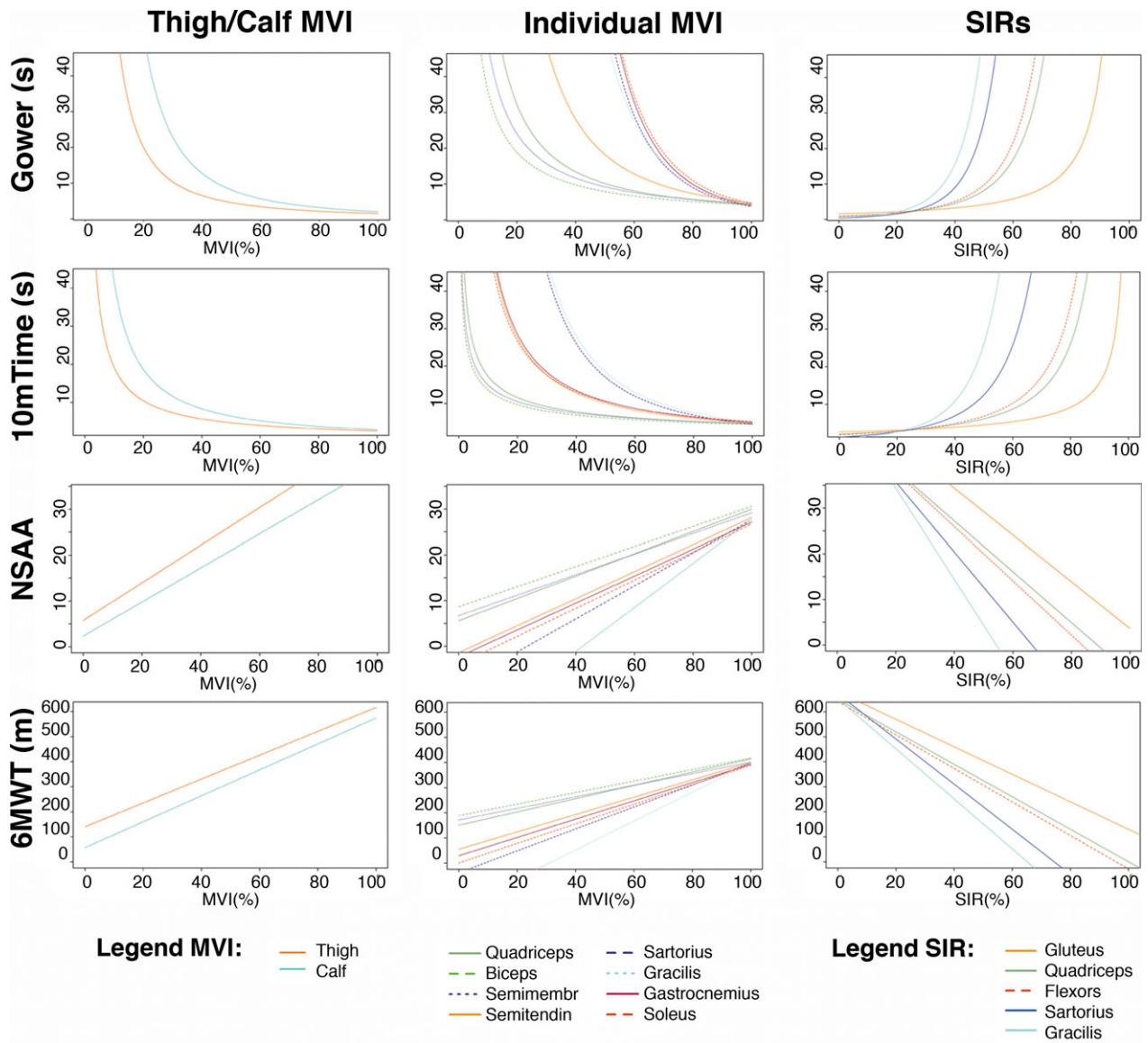
Figure 8. Correlation and regression analyses among MRI parameters and clinical scores. We performed correlation and regression analyses of functional tests (Gowers in upper row, 10-m walking time in second row, North Star Ambulatory Assessment (NSAA) in third row, 6-min walking test in lower row) and MRI parameters (thigh/calf MVIs in left column, individual MVI in central column and SIRs in right column). All analyses resulted statistically significant ($P < 0.05$), with the best correlation coefficient found between MRI parameters and NSAA (Spearman $\rho ho = 0.7$–0.8). We found a linear regression between MRI parameters and NSAA and 6MWT, and an inverse relationship existing between time-related tests (Gowers, 10mTime) and MVIs (thigh/calf or individual). Gowers and 10 m walking time could be predicted by SIRs through a positive nonlinear growth function. Interestingly, a recurrent clustering of different muscles in predicting the outcome of functional tests (quadriceps-biceps-semimembranosus, semintendinosus, sartorius-gracilis) was observed, thus suggesting a multi-step model of muscular involvement in Duchenne muscular dystrophy. MVI, muscle volume index; SIR, signal intensity ratio; 10mTime, 10-m time; NSAA, North Star Ambulatory Assessment; 6MWT, 6-min walking test.

weight, and BMI growth. These curves are supported by data from up to 4-year serial imaging of the pelvic girdle, thighs, and calves, corresponding to the most comprehensive quantitative evaluation performed with MRI so far. Reference curves could turn out to be important for future experimental studies. Furthermore, the different

slopes of unaffected muscle volume reduction relative to age also suggests that in cohort of DMD patients of different ages diverse muscles can work as "sentinel muscles" being more able to show treatment-induced changes in a given temporal frame. For example, MRI-derived measures of the glutei, biceps, and quadriceps are more

sensitive to disease progression during the 5–8 age groups, whereas the measurement of sartorius, gracilis soleus, and gastrocnemius could be important in older patients.

Both T1 SIRs and MVIs showed significant correlations with all clinical measures. Interestingly, different clinical tests showed different morpho-functional linkage to different groups of muscles, disclosing important contributions of the calves to 10-m time and other endurance outcomes, but not to Gowers. The provided morpho-functional associations (linear, inverse or exponential) allow calculating an expected clinical value relative to fat infiltration and volume measures, independently from patients' age.

Finally, muscle SIRs and MVIs progressively worsened over time even in nonambulant patients, in which time-tests cannot be performed, suggesting the clinical usefulness of this quantitative MRI measure also in advanced stages of the disease. Clinical test specifically developed for nonambulant DMD patients were not performed, since it was beyond the scope of this study. Cut-off values of qMRI parameters allowing discrimination between ambulant and not-ambulant patients could be identified, with up to 100% accuracy.

In conclusion, quantitative MRI permits a sensitive and objective assessment of individual muscle composition, in opposition to gross measures of functional tests, but can also provide information on many muscles in their entirety, as opposed to muscle biopsy. Quantitative MRI can show the multi-step process of involvement of muscles in the lower limbs of DMD patients, displaying the natural history of disease in different muscles and allowing monitoring disease progression also in nonambulant patient. Our study provides a fundamental quantitative reference background for future experimental studies on new therapies. Ultimately, given the great heterogeneity of DMD severity according to age, the use of quantitative MRI should be encouraged not only in research, but also in clinical settings.

Author Contribution

LSP, CG, FC, SCP, RG, GC, and YT have collaborated in conception and design of the study. LSP, CG, AA, CSa, AI, SG, and AF contributed to acquisition and analysis of the images and of data. MFN, SCP, MGNS, SN, MS, AT, MPC, CSi, MV, and FC collaborated in clinical management of the patients. CG, AA, and LSP contributed to manuscript and figures preparation.

Conflict of Interest

All authors have nothing to disclose.

References

1. Emery AEH. The muscular dystrophies. Lancet 2002;359:687–695.

2. Bushby K, Finkel R, Birnkrant DJ, et al. Diagnosis and management of Duchenne muscular dystrophy, part 1: diagnosis, and pharmacological and psychosocial management. Lancet Neurol 2010;9:77–93.

3. Petrof BJ. Molecular pathophysiology of myofiber injury in deficiencies of the dystrophin-glycoprotein complex. Am J Phys Med Rehabil 2002;81(11 Suppl):S162–S174.

4. Cossu G, Sampaolesi M. New therapies for Duchenne muscular dystrophy: challenges, prospects and clinical trials. Trends Mol Med 2007;13:520–526.

5. Harper SQ, Hauser MA, DelloRusso C, et al. Modular flexibility of dystrophin: implications for gene therapy of Duchenne muscular dystrophy. Nat Med 2002;8:253–261.

6. Wein N, Vulin A, Falzarano MS, et al. Translation from a DMD exon 5 IRES results in a functional dystrophin isoform that attenuates dystrophinopathy in humans and mice. Nat Med 2014;20:992–1000.

7. Mann CJ, Honeyman K, Cheng AJ, et al. Antisense-induced exon skipping and synthesis of dystrophin in the mdx mouse. Proc Natl Acad Sci USA 2001;98:42–47.

8. De Angelis FG, Sthandier O, Berarducci B, et al. Chimeric snRNA molecules carrying antisense sequences against the splice junctions of exon 51 of the dystrophin pre-mRNA induce exon skipping and restoration of a dystrophin synthesis in Delta 48–50 DMD cells. Proc Natl Acad Sci USA 2002;99:9456–9461.

9. Sampaolesi M, Torrente Y, Innocenzi A, et al. Cell therapy of alpha-sarcoglycan null dystrophic mice through intra-arterial delivery of mesoangioblasts. Science 2003;301:487–492.

10. Sampaolesi M, Blot S, D'Antona G, et al. Mesoangioblast stem cells ameliorate muscle function in dystrophic dogs. Nature 2006;444:574–579.

11. Schreiber A, Smith W, Ionasescu V, et al. Magnetic resonance imaging of children with Duchenne muscular dystrophy. Pediatr Radiol 1987;17:495–497.

12. Kinali M, Arechavala-Gomeza V, Cirak S, et al. Muscle histology vs MRI in Duchenne muscular dystrophy. Neurology 2011;76:346–353.

13. Liu G-C, Jong Y-J, Chiang C-H, Jaw T-S. Duchenne muscular dystrophy: MR grading system with functional correlation. Radiology 1993;186:475–480.

14. Kim HK, Laor T, Horn PS, et al. T2 mapping in duchenne muscular dystrophy: distribution of disease activity and correlation with clinical assessments. Radiology 2010a;255:899–908.

15. Forbes S, Walter G, Rooney WD, et al. Skeletal muscles of ambulant children with duchenne muscular dystrophy: validation of multicenter study of evaluation with MR Imaging and MR spectroscopy. Radiology 2013;269:198–207.

16. Garrood P, Hollingsworth KG, Eagle M, et al. MR imaging in duchenne muscular dystrophy: quantification of T1-weighted signal, contrast uptake, and the effects of exercise. J Magn Reson Imaging 2009;1138:1130–1138.

17. Hollingsworth KG, Garrood P, Eagle M, et al. Magnetic resonance imaging in Duchenne muscular dystrophy: longitudinal assessment of natural history over 18 months. Muscle Nerve 2013;48:586–588.

18. Senesac CR, Lott DJ, Forbes SC, et al. Longitudinal evaluation of muscle composition using magnetic resonance in 4 boys with Duchenne muscular dystrophy: case series. Phys Ther 2015;95:978–988.

19. Arpan I, Willcocks RJ, Forbes SC, et al. Examination of effects of corticosteroids on skeletal muscles of boys with DMD using MRI and MRS. Neurology 2014;83:974–980.

20. Willcocks RJ, Arpan IA, Forbes SC, et al. Longitudinal measurements of MRI-T2 in boys with Duchenne muscular dystrophy: effects of age and disease progression. Neuromuscul Disord 2014;24:393–401.

21. Kim HK, Laor T, Horn PS, et al. Quantitative assessment of the T2 relaxation time of the gluteus muscles in children with Duchenne muscular dystrophy: a comparative study before and after steroid treatment. Korean J Radiol 2010b;11:304–311.

22. Lerario A, Bonfiglio S, Sormani M, et al. Quantitative muscle strength assessment in duchenne muscular dystrophy: longitudinal study and correlation with functional measures. BMC Neurol 2012;12:91.

23. Mercuri E, Pichiecchio A, Allsop J, et al. Muscle MRI in inherited neuromuscular disorders: past, present, and future. J Magn Reson Imaging 2007;25:433–440.

24. Marden FA, Connolly AM, Siegel MJ, Rubin DA. Compositional analysis of muscle in boys with Duchenne muscular dystrophy using MR imaging. Skeletal Radiol 2005;34:140–148.

25. Gaeta M, Messina S, Mileto A, et al. Muscle fat-fraction and mapping in Duchenne muscular dystrophy: evaluation of disease distribution and correlation with clinical assessments. Preliminary experience. Skelet Radiol 2012;41:955–961.

26. Albracht K, Arampatzis A, Baltzopoulos V. Assessment of muscle volume and physiological cross-sectional area of the human triceps surae muscle in vivo. J Biomech 2008;41:2211–2218.

27. Akagi R, Takai Y, Ohta M, et al. Muscle volume compared to cross-sectional area is more appropriate for evaluating muscle strength in young and elderly individuals. Age Ageing 2009;38:564–569.

28. O'Brien TD, Reeves ND, Baltzopoulos V, et al. Strong relationships exist between muscle volume, joint power and whole-body external mechanical power in adults and children. Exp Physiol 2009;94:731–738.

29. Wokke BH, Bos C, Reijnierse M, et al. Comparison of dixon and T1-weighted MR methods to assess the degree of fat infiltration in duchenne muscular dystrophy patients. J Magn Reson Imaging 2013;38:619–624.

30. Wren T, Bluml S, Tseng-Ong L, Gilsanz V. Three-point technique of fat a marker of disease progression in Duchenne muscular dystrophy: preliminary study. AJR 2008;190:8–12.

Supporting Information

Additional Supporting Information may be found online in the supporting information tab for this article:

Figure S1. Progression of quantitative MRI parameters after loss of ambulation. The progressive increase in SIRs (A) and the progressive decrease in MVIs (B-C) in the six patients that became wheel chair-bound during the study before and after loss of ambulation are reported. Time is shown in years. SIR, signal intensity ratio; MVI, muscle volume index.

Figure S2. ROC curves of quantitative MRI parameters for discrimination of ambulation ability in Duchenne muscular dystrophy patients. ROC curves of quadriceps SIR (A), flexors SIR (B), thigh MVI (C), calf MVI (D), biceps MVI (E), and soleus MVI (F) are reported, showing high sensitivity and specificity in discrimination of ambulant and wheel chair-bound patients. SIR, signal intensity ratio; MVI, muscle volume index.

Figure S3. Age-related reference curves of clinical tests and force measurements. Age-related quantiles were calculated and plotted for 6MWT (A), NSAA (B), 10-m walking time (C), Gowers (D), extensor iso-kinetic contraction (E), extensor iso-metric contraction (F), flexor iso-kinetic contraction (G), and flexor iso-metric contraction (H). Please note the high variability among patients (see 5th and 95th percentile lines) of all clinical tests and force measurements. 6MWT, 6-min walking test; NSAA, North Star Ambulatory Assessment.